State-dependent block of Orai3 TM1 and TM3 cysteine mutants: Insights into 2-APB activation

Anna Amcheslavsky, Olga Safrina, and Michael D. Cahalan

Department of Physiology and Biophysics, University of California, Irvine, Irvine, CA 92697

After endoplasmic reticulum (ER) Ca^{2+} store depletion, Orai channels in the plasma membrane (PM) are activated directly by ER-resident stromal interacting molecule (STIM) proteins to form the Ca^{2+}-selective Ca^{2+} release-activated Ca^{2+} (CRAC) channel. Of the three human Orai channel homologues, only Orai3 can be activated by high concentrations (>50 µM) of 2-aminoethyl diphenylborinate (2-APB). 2-APB activation of Orai3 occurs without STIM1–Orai3 interaction or store depletion, and results in a cationic, nonselective current characterized by biphasic inward and outward rectification. Here we use cysteine scanning mutagenesis, thiol-reactive reagents, and patch-clamp analysis to define the residues that assist in formation of the 2-APB–activated Orai3 pore. Mutating transmembrane (TM) 1 residues Q83, V77, and L70 to cysteine results in potentiated block by cadmium ions (Cd^{2+}). TM1 mutants E81C, G73A, G73C, and R66C form channels that are not sensitive to 2-APB activation. We also find that Orai3 mutant V77C is sensitive to block by 2-aminoethyl methanethiosulfonate (MTSEA), but not 2-(trimethylammonium)ethyl methanethiosulfonate (MTSET). Block induced by reaction with MTSEA is state dependent, as it occurs only when Orai3-V77C channels are opened by either 2-APB or by cotransfection with STIM1 and concurrent passive store depletion. We also analyzed TM3 residue E165. Mutation E165A in Orai3 results in diminished 2-APB–activated currents. However, it has little effect on store-operated current density. Furthermore, mutation E165C results in Cd^{2+}-induced block that is state dependent: Cd^{2+} only blocks 2-APB–activated, not store-operated, mutant channels. Our data suggest that the dilated pore of 2-APB–activated Orai3 is lined by TM1 residues, but also allows for TM3 E165 to approach the central axis of the channel that forms the conducting pathway, or pore.

The Journal of General Physiology

INTRODUCTION

Store-operated calcium entry (SOCE) is the process by which calcium ions (Ca^{2+}) enter cells after ER Ca^{2+} store depletion. SOCE increases cytosolic Ca^{2+} concentrations, refills cellular Ca^{2+} stores, and triggers signaling cascades responsible for secretion, gene transcription, alterations in motility, and cell proliferation (Putney, 1986; Bootman et al., 2001; Parekh and Putney, 2005; Cahalan, 2009). A succession of RNAi screens led to the molecular identification of stromal interacting molecule (STIM) and Orai, the two proteins that underlie SOCE in multiple cell types (Liou et al., 2005; Roos et al., 2005; Zhang et al., 2005; Feske et al., 2006; Vig et al., 2006b). ER membrane–resident STIM proteins sense Ca^{2+} store depletion and translocate to cortical ER–plasma membrane (PM) junctions, where they physically interact with and activate the PM-bound Orai pore-forming subunits (Liou et al., 2005; Zhang et al., 2005; Prakriya et al., 2006; Vig et al., 2006b; Yeromin et al., 2006; Cahalan, 2009; Soboloff et al., 2012). There are two mammalian homologues of STIM: STIM1 and STIM2; and three mammalian homologues of Orai: Orai1, Orai2, and Orai3. Together, STIM1 and Orai1 form the highly Ca^{2+}-selective Ca^{2+} release-activated Ca^{2+} (CRAC) channel of T lymphocytes.

The molecular identification of Orai1 led to a plethora of mutagenesis studies that identified key residues in transmembrane (TM) 1 involved in conduction and gating of the CRAC channel. These residues are conserved among human Orai homologues, and most are present in *Drosophila melanogaster* Orai (dOrai) as well. The first of these studies identified an Orai1 R91W mutation in patients afflicted with severe combined immune deficiency (SCID; Feske et al., 2006). The R91 residue is localized toward the intracellular side of TM1; mutating it to various bulky hydrophobic residues results in channel block, whereas mutating it to hydrophilic residues maintains channel function (Derler et al., 2009; Zhang et al., 2011). Therefore, R91 (R66 in Orai3 and K165 in dOrai) has been implicated in channel gating. The glutamate toward the extracellular side of TM1 (E106 in Orai1, E81 in Orai3, and E180 in dOrai) was identified

Correspondence to Michael D. Cahalan: mcahalan@uci.edu

Abbreviations used in this paper: 2-APB, 2-aminoethyl diphenylborinate; BMS, bis(2-mercaptoethylsulfone); CRAC, Ca^{2+} release-activated Ca^{2+}; HEK, human embryonic kidney; MTSEA, 2-aminoethyl methanethiosulfonate; MTSTEAE, 2-(triethylammonium)ethyl methanethiosulfonate; MTSET, 2-(trimethylammonium)ethyl methanethiosulfonate; PM, plasma membrane; SOCE, store-operated calcium entry; STIM, stromal interacting molecule; WT, wild type.

The Rockefeller University Press $30.00
J. Gen. Physiol. Vol. 143 No. 5 621–631
www.jgp.org/cgi/doi/10.1085/jgp.201411171

as the channel's selectivity filter (Prakriya et al., 2006; Vig et al., 2006a; Yeromin et al., 2006). Two cysteine scanning mutagenesis studies, one functional (McNally et al., 2009) and one biochemical (Zhou et al., 2010) in nature, concluded that residues lining an α-helical Orai1 TM1 domain form the conduction pathway of the channel. These residues included E106, V102, G98, L95, R91, and A88. Later studies identified G98 as the channel's "gating hinge" (Zhang et al., 2011) and V102 as its hydrophobic gate (McNally et al., 2012). All of these discoveries were then substantiated by the solved dOrai crystal structure (Hou et al., 2012).

Orai3, like Orai1, can be activated by store depletion and STIM1 interaction (Lis et al., 2007). Due to its high homology, the store-operated pore of Orai3 is thought to be similar to the store-operated pore of Orai1. Interestingly, Orai3 can also be activated by 2-aminoethyl diphenylborinate (2-APB), bypassing the need for store depletion and STIM1 interaction (DeHaven et al., 2008; Peinelt et al., 2008; Zhang et al., 2008). In fact, 2-APB and STIM1 antagonize each other as Orai3 channel activators; STIM1-bound Orai3 channels resist 2-APB activation, whereas 2-APB–activated channels resist STIM1-induced channel opening (Yamashita et al., 2011). Furthermore, 2-APB activates Orai3 by opening and dilating the conducting pore (Schindl et al., 2008), resulting in a nonselective, inwardly and outwardly rectifying cationic current that biophysically differs from the store-operated (STIM1-activated) Orai3 current. Chimeras composed of both Orai1 and Orai3 subdomains have shown that the TM2-TM3 region of Orai3 is necessary for activation by 2-APB (Zhang et al., 2008). Additionally, mutation G183A in TM3 of Orai1 results in Orai1 channels that can also be activated by 2-APB; and mutating the homologous G158 in TM3 of Orai3 to cysteine results in slowed kinetics of 2-APB activation and washout due to disulfide bridge formation between the introduced G158C and endogenous TM2 C101 (Amcheslavsky et al., 2013). Collectively, these data suggest that 2-APB activates Orai3 by interacting within the TM2-TM3 region proximal to the conserved glycine present at the center of TM3 of Orai homologues. However, a complete understanding of the 2-APB–activated Orai3 pore domain is lacking.

Here, we use targeted cysteine mutagenesis, thiol-reactive reagents, and patch-clamp analysis to identify a subset of residues that assist in formation of the 2-APB–activated Orai3 pore. We focus on specific TM1 residues that are known to line the pores of store-operated Orai1 channels (McNally et al., 2009; Zhou et al., 2010). We then examine TM3 E165, a conserved TM3 residue that has been shown to affect Ca^{2+} selectivity in STIM1-operated Orai1 and 2-APB–activated Orai3 (Prakriya et al., 2006; Schindl et al., 2008). We show that particular TM1 and TM3 cysteine mutants exhibit state-dependent block of current by $CdCl_2$ and/or 2-aminoethyl methanethiosulfonate (MTSEA) and discuss our results in the context of the published dOrai crystal structure (Hou et al., 2012).

MATERIALS AND METHODS

Please see Amcheslavsky et al. (2013) for detailed protocols. The following are brief explanations.

Molecular biology

Human Myc-STIM1 in vector pCI, as previously described by Roos et al. (2005) and Lioudyno et al. (2008), was used in experiments involving store-operated currents. An EGFP-Orai3-WT construct was used both as a wild-type (WT) control and as a template for generating mutant Orai3 channel constructs. For simplicity, "EGFP" is omitted from construct names throughout the text.

List of primers

E81C: forward, 5′-CCATGGTGGCCATGGTGTGCGTGCAGCTGGAGAGTG-3′; reverse, 5′-CACTCTCCAGCTGCACGCACACCATGGCCACCATGG-3′. Q83C: forward, 5′-GCCATGGTGGAGGTGTGCCTGGAGAGTGACCACG-3′; reverse, 5′-CGTGGTCACTCTCCAGGCACACCTCCACCATGGC-3′. V77C: forward, 5′-CTCGGGCTTCGCCATGTGTGCCATGGTGGAGGTG-3′; reverse, 5′-CACCTCCACCATGGCACACATGGCGAAGCCCGAG-3′. G73C: forward, 5′-CTGCCTTGCTCTCGTGCTTCGCCATGGTG-3′; reverse, 5′-CACCATGGCGAAGCACGAGAGCAAGGCAG-3′. G73A: forward, 5′-GCCTTGCTCTCGGCCTTCGCCATGGTG-3′; reverse: 5′-CACCATGGCGAAGGCCGAGAGCAAGGC-3′. L70C: forward, 5′-CCGCACGTCTGCCTGTCTCTCGGGCTTCG-3′; reverse, 5′-CGAAGCCCGAGAGACAGGCAGACGTGCGG-3′. R66C: forward: 5′-CTCAAAGCTTCCAGCTGCACGTCTGCCTTG-3′; reverse, 5′-CAAGGCAGACGTGCAGCTGGAAGCTTTGAG-3′. E165A: forward, 5′-CTTTCTCTTCCTTGCTGCAGTTGTCCTGGTTGG-3′; reverse, 5′-CCAACCAGGACAACTGCAGCAAGGAAGAGAAAG-3′. E165C: forward: 5′-CACCTTTCTCTTCCTTGCTTGCGTTGTCCTGGTTGGTTGG-3′; reverse: 5′-CCAACCAACCAGGACAACGCAAGCAAGGAAGAGAAAGGTG-3′. Sequencing: forward, 5′-CATGGTCCTGCTGGAGTTCGTG-3′; reverse, 5′-CCTCTACAAATGTGGTATGG-3′.

Cell culture

Human embryonic kidney (HEK) 293A cells (Invitrogen) were incubated at 37°C, 5% CO_2, and maintained in Dulbecco's modified Eagle's medium (DMEM; Lonza) supplemented with 10% fetal calf serum (Omega Scientific) and 2 mM L-glutamine (Sigma-Aldrich). For experiments, cells were plated onto 6-well plate dishes and given 24–72 h to grow to ∼95% confluency for transfection in Lipofectamine 2000 (catalogue No. 11668-019; Invitrogen), as advised by Invitrogen, with OPTI-MEM I (1×; Gibco; Life Technologies). For experiments involving 2-APB–activated currents, an Orai3 construct alone was transfected into HEK cells. For experiments involving store-operated currents, myc-STIM1 and an Orai3 construct of choice were both transfected into HEK cells (transfection ratio of 2:1 of STIM1 to Orai3).

Electrophysiology

Transfected HEK 293A cells were chosen for whole-cell recording by expression of EGFP, 48 h after transfection. Patch-clamp experiments were performed at room temperature with standard whole-cell recording. Patch pipettes had ∼2 MΩ resistances. Only cells with high input resistance (>1 GΩ) were recorded from. The series resistance (2–7 MΩ) was compensated by 80%. Membrane potentials were corrected for the liquid junction potential of 10 mV. Currents were recorded using an EPC-9 patch-clamp amplifier (HEKA). Data were acquired by PULSE software (HEKA) and were digitally filtered at 1 kHz for analysis and display. Our

protocol alternates voltage ramps lasting 220 ms from −120 to 100 mV and pulses of 220 ms to −120 mV every 2 s from a holding potential of 0 mV. Time courses represent inward and outward currents recorded at −120 and +100 mV, respectively. Five current-voltage (I-V) curves were averaged for display. In experiments involving 2-APB–activated currents, current before channel activation was used for leak subtraction. In experiments involving store-operated currents, current during application of 50 µM $LaCl_3$ or 10 µM $GdCl_3$ was used for leak subtraction. Unless otherwise stated, leak-subtracted I-V curves are displayed. Data were analyzed and graphed in OriginPro 7.5. The following equation was used to generate $CdCl_2$ dose–response curves represented in Figs. 1 and 5:

$$y = MIN + (MAX - MIN) \times x^n / (k^n + x^n),$$

where *MIN* and *MAX* are the minimum and maximum current values, respectively, *k* is concentration at which 50% of current is blocked, and *n* is the number of cooperative sites. Parameters were not fixed during analysis. Curves of best fit were chosen for representation.

All external solutions were pH adjusted to 7.4 by NaOH or CsOH and have osmolality adjusted to 325 mosm/kg by sucrose. 2-APB, bis(2-mercaptoethylsulfone) (BMS), MTS reagents, $CdCl_2$, $LaCl_3$, and/or $GdCl_3$ were added to Ringer's solution as needed. Compositions of external solutions are described in Table 1.

Final concentrations of various additives used throughout the paper were as follows: 100 µM 2-APB, 5 mM BMS, 1 mM MTSEA, 1 mM 2-(trimethylammonium)ethyl methanethiosulfonate (MTSET), 500 µM 2-(triethylammonium)ethyl methanethiosulfonate (MTSTEAE), varied $CdCl_2$ (as described in the main text and figures), 50 µM $LaCl_3$, and 10 µM $GdCl_3$. MTS reagents were purchased from Toronto Research Chemicals (catalog Nos. A609100, T795900, and T775800 for MTSEA, MTSET, and MTSTEAE, respectively).

The internal solution for experiments involving 2-APB–activated currents consisted of (in mM): 144 CsAsp, 8 magnesium $gluconate_2$, 2 CsCl, 15 HEPES, 12 Cs_4EGTA, and 2.5 $Ca(OH)_2$, pH adjusted to 7.2 by CsOH, with a free $[Ca^{2+}]$ of 50 nM (calculated by Maxchelator, available online) and osmolality of 330 mosm/kg. The internal solution for experiments involving store-operated currents consisted of (in mM): 138 CsAsp, 8 Mg-$gluconate_2$, 2 CsCl, 15 HEPES, 10 Cs_4BAPTA, pH adjusted to 7.2 by CsOH, and 20 µM inositol 1,4,5 trisphosphate (IP_3; added fresh on the day of the experiment from 10 mM stock; catalogue No. 10008205; Cayman Chemical Company).

Online supplemental material

Fig. S1 summarizes current densities of Orai3 TM1 cysteine mutants insensitive to 2-APB activation, compared with current density of Orai3-WT channels. Fig. S2 summarizes MTS reagent effects on 2-APB–activated Orai3-Q83C and Orai3-L70C mutant channels. Fig. S3 shows that MTSEA and MTSET reagents do not block 2-APB-activated Orai3-E165C channels. Online supplemental material is available at http://www.jgp.org/cgi/content/full/jgp.201411171/DC1.

RESULTS

Select TM1 cysteine mutants are sensitive to $CdCl_2$ block during 2-APB activation

To determine whether the TM1 residues known to line the store-operated Orai1 pore are involved in the formation of the 2-APB–activated Orai3 pore, we introduced cysteine mutations into homologous positions—Q83, E81, V77, G73, L70, and R66—of the Orai3 protein. We then performed a series of experiments in which we first activated these mutant Orai3 channels with 2-APB and then attempted to block with varying concentrations of $CdCl_2$. We hypothesized that electrostatic interactions between Cd^{2+} and accessible sulfhydryl groups of introduced cysteines within the Orai3 pore would result in channel block. First, we compared $CdCl_2$ sensitivity in WT and mutant Orai3 channels and found that Orai3-WT channels required higher concentrations of $CdCl_2$ to block 2-APB–activated current ($n = 10$) than do Orai3-Q83C ($n = 4$), Orai3-V77C ($n = 6$), and Orai3-L70C ($n = 4$) mutant channels. Representative time courses and corresponding I-V relationships taken from $CdCl_2$ block experiments for Orai3-WT, Orai3-Q83C, Orai3-V77C, and Orai3-L70C are shown in Fig. 1 (A–H). $CdCl_2$ dose–response curves for both inward and outward components of 2-APB–activated Orai3-WT, Orai3-Q83C, Orai3-V77C, and Orai3-L70C current are represented in Fig. 1 (I and J) and show current remaining upon application of corresponding $CdCl_2$ concentration. These dose–response curves show that mutations Q83C,

TABLE 1

Compositions of external solutions

Chemical	2 Ca (Ringer's)	20 Ca	2 CaChol	20 CaChol	NaDVF	CsDVF
NaCl	151.5	120	–	–	160	–
CsCl	–	–	–	–	–	160
KCl	4.5	–	–	–	–	–
$CaCl_2$	2	20	2	20	–	–
Choline-Cl	–	–	156	120	–	–
HEDTA	–	–	–	–	2	2
HEPES	10	10	10	10	10	10
Glucose	10	10	10	10	10	10
Sucrose	11	26	14	31	1	11
pH adjusted to 7.2 by	NaOH	NaOH	Choline-OH	Choline-OH	NaOH	CsOH

Compositions of external solutions used during patch clamp experiments. Numbers represent concentrations (in mM). DVF, divalent free. –, not applicable.

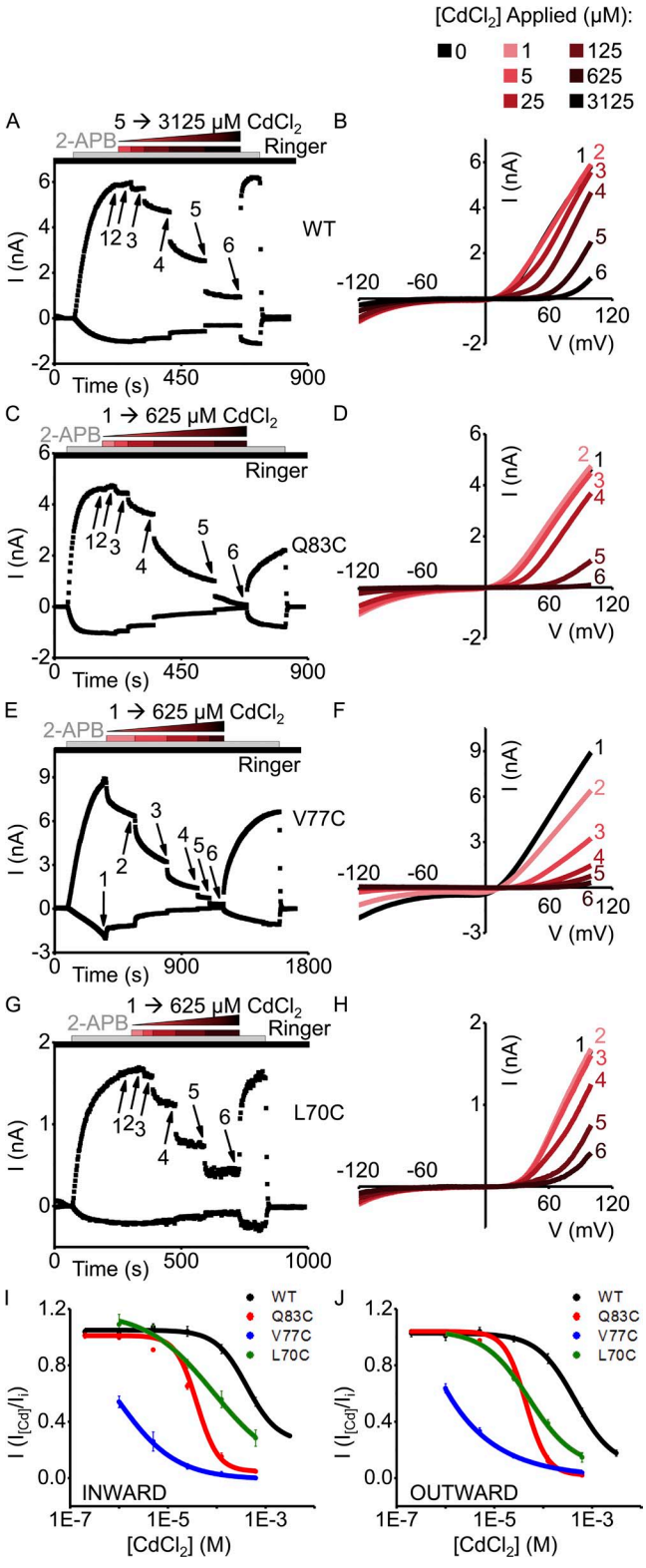

Figure 1. Select TM1 cysteine mutants are sensitive to $CdCl_2$ block during 2-APB activation. (A, C, E, and G) Time courses for Orai3-WT, Orai3-Q83C, Orai3-V77C, and Orai3-L70C, respectively (WT, $n = 10$; Q83C, $n = 4$; V77C, $n = 6$; L70C, $n = 4$), represented as current amplitude (nA) versus time (s), activated by 100 μM 2-APB, and blocked by indicated concentrations of $CdCl_2$. Note that [$CdCl_2$] used to block WT channels ranges from 5 μM to 3.125 mM, whereas [$CdCl_2$] used to block mutant channels ranges from only 5 to 625 μM. (B, D, F, and H) I-V relationships corresponding to time points indicated by arrows in A, C, E, and G, respectively. (I and J) Fraction of 2-APB–activated inward and outward currents, respectively, remaining upon applied concentration of $CdCl_2$. Calculated K_d values for $CdCl_2$ block of inward currents carried by WT, Q83C, V77C, and L70C are as follows: 734, 41.8, 1.22, and 156 μM, respectively. Calculated K_d values for $CdCl_2$ block of outward currents carried by WT, Q83C, V77C, and L70C are as follows: 549, 64.3, 1.72, and 67.3 μM, respectively. Data points were gathered from experiments represented in A–H, and curves are sigmoidal fits of data points. Data points are represented as $I_{[Cd]}/I_i$, where $I_{[Cd]}$ is current recorded after application of $CdCl_2$ and I_i is current recorded before application of $CdCl_2$. Error bars indicate SEM.

V77C, and L70C potentiate sensitivity to $CdCl_2$ block. Therefore, residues Q83, V77, and L70 are involved in the formation of the 2-APB–activated Orai3 pore.

Mutant channels Orai3-E81C, Orai3-G73A, Orai3-G73C, and Orai3-R66C failed to activate upon 2-APB application during whole-cell experiments (2-APB–activated current densities remained well below 3 pA/pF, >100-fold less than that of WT current density). Treatment with reducing reagent BMS during 2-APB activation of Orai3-G73C and Orai3-R66C mutant channels did not increase current amplitude. This result, along with nonfunctional G73A channels, suggests that mutations G73C and R66C alter Orai3 sensitivity to 2-APB activation or prevent the formation of a conducting pore. The lack of response to 2-APB application is not the result of block due to intersubunit disulfide bridge formation, which might block the conducting 2-APB–activated Orai3 pathway. These data are summarized in Fig. S1 by bar graphs representing current density carried by mutants compared with Orai3-WT channels.

State-dependent block of 2-APB–activated Orai3-V77C mutant channels by MTSEA

MTS reagents are thiol-reactive probes that react with accessible cysteine sulfhydryl by covalent linkage. If an MTS reagent covalently binds to a cysteine residue within the conduction pathway, or pore, of an ion channel, channel conduction is blocked until the interaction is reversed by use of a reducing reagent, such as BMS. In our next set of experiments, we sought to test the Cd^{2+}-sensitive TM1 cysteine mutants described in the previous section of our results for block by positively charged MTS reagents. We found that MTSEA ($n = 3$), MTSET ($n = 3$), and MTSEAE ($n = 3$) only reversibly blocked 2-APB–activated Orai3-WT channels (Fig. 2, A and B; and Fig. S2, A and B). Therefore, the four endogenous Orai3 cysteines, two in TM2 and two in the TM3-TM4 loop, either did not react with applied MTS reagents or did not react in such a way as to result in irreversible channel block. Similarly, BMS application results in partial inhibition of 2-APB–activated Orai3

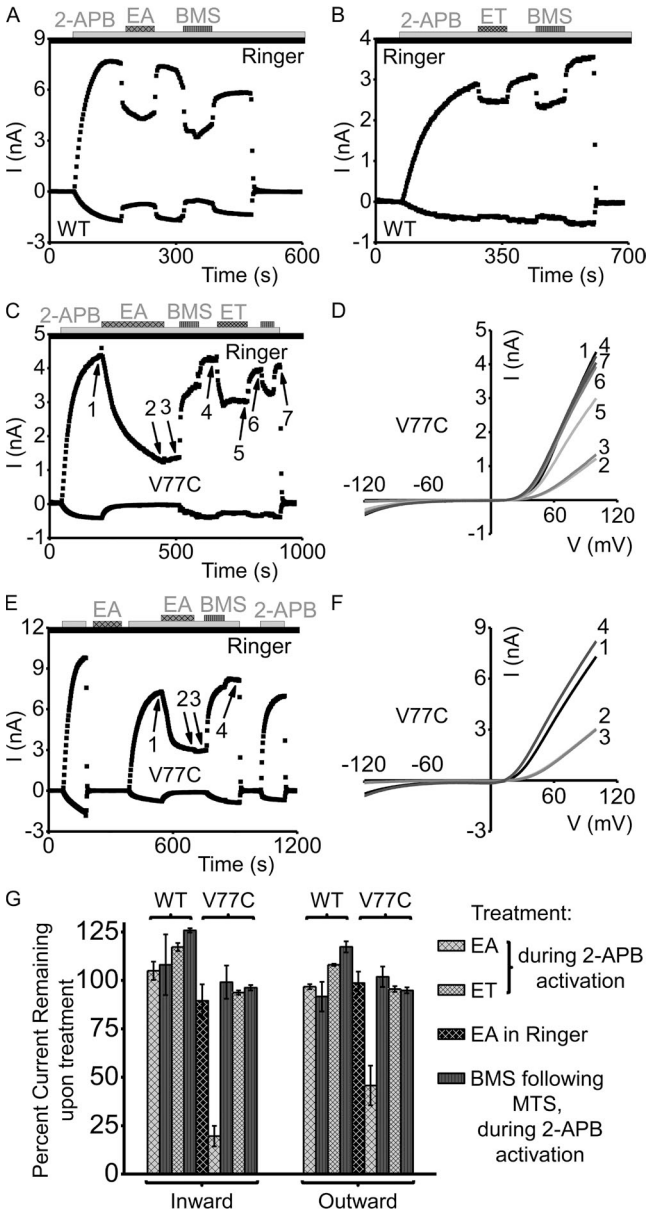

Figure 2. State-dependent block of 2-APB–activated Orai3-V77C mutant channels by MTS reagents. (A and B) Time courses for control Orai3-WT (WT) currents. Channels were activated by 100 µM 2-APB; subsequent application of cationic MTS reagents MTSEA (EA; n = 3) and MTSET (ET; n = 3) did not induce irreversible block of current. BMS application reversibly inhibits current. (C) Time course for Orai3-V77C (V77C; n = 3) currents activated by 100 µM 2-APB. Subsequent application of EA (n = 3), but not ET (n = 3), results in an irreversible block of current. Application of BMS reverses EA-induced block. (D) I-V relationships corresponding to currents recorded at time points indicated by the arrows in C. (E) Time course for Orai3-V77C (V77C) activated by 100 µM 2-APB. EA was applied during Ringer perfusion or during 2-APB activation. EA blocks only the open state of Orai3-V77C channels. (F) I-V relationships corresponding to currents recorded at time points indicated by the arrows in E. (G) Bar graphs summarizing the percentage of current remaining of both inward and outward components of 2-APB–activated current carried by WT or V77C channels. The percentage of current remaining upon application and washout of EA or ET, and subsequent application and washout of BMS, is represented. A bar graph showing lack of V77C block by EA application during Ringer's perfusion is also represented. Data are normalized to current amplitude before initial MTS reagent application. Error bars indicate SEM.

current. 2-APB–activated Orai3-V77C channels, however, behaved differently. Almost 80% of current through Orai3-V77C was blocked by MTSEA (n = 3) and remained blocked after washout. Current amplitudes only returned to normal upon subsequent application and washout of BMS. Additionally, the larger MTSET did not block current through Orai3-V77C (n = 3; Fig. 2, C and D). To test the state dependence of the MTSEA block, we applied MTSEA to Orai3-V77C channels during Ringer perfusion, as opposed to during 2-APB activation, and found that it did not result in channel block (Fig. 2, E and F). Thus, only the Orai3-V77C open state pore is wide enough to allow MTSEA, but not MTSET, to penetrate, to react covalently with the introduced cysteine residue, and to block current. These data are summarized as bar graphs in terms of percentage of current remaining upon treatment with an MTS reagent, with or without BMS, in Fig. 2 G. Our data show that residue V77 is positioned within the 2-APB–activated Orai3 pore and that when mutated to cysteine, its reaction with MTSEA forms a plug that directly inhibits conduction. Finally, like Orai3-WT channels, Orai3-Q83C and Orai3-L70C channels were resistant to irreversible block by MTSEA, MTSET, or MTSTEAE (Fig. S2).

Store-operated Orai3-V77C channels are sensitive to block by MTSEA

In the next set of experiments, we sought to test whether the more selective, store-operated Orai3 pore is physically narrower than the 2-APB–activated Orai3 pore by using MTSEA as a probe. Store-operated Orai3-WT channels exhibited only reversible block of current by MTSEA; upon reagent washout, currents increased to amplitudes recorded before MTSEA application (n = 3; Fig. 3, A and B). Again, endogenous Orai3 cysteines did not react with MTSEA or at least did not react in such a way as to inhibit conduction. However, to our surprise, store-operated Orai3-V77C current was blocked by MTSEA and remained blocked upon washout of the reagent (n = 8). Orai3-V77C current amplitudes only returned to normal upon application of BMS (Fig. 3, C and D). Overall, on average 55% of store-operated current through Orai3-V77C channels was blocked by application of MTSEA (Fig. 3 E). Although MTSEA blocks a greater percentage of 2-APB–activated Orai3 current (~80%), our data suggest that residue V77 is directly involved in the formation of both the 2-APB–activated and the store-operated (STIM1-activated)

Orai3 pore. Perhaps the greater extent of block exhibited during 2-APB activation, as opposed to STIM1-induced activation, can be explained by the larger diameter of the dilated 2-APB–activated Orai3 pore.

Orai3-E165A exhibits diminished 2-APB–activated, but normal store-operated, current densities

In the next set of experiments, we sought to determine the role of the Orai3 TM3 E165 residue in pore formation. As discussed in the introduction, E165 and its homologue E190 of Orai1 have been shown to effect Ca^{2+} selectivity and 2-APB gating (Prakriya et al., 2006; Vig et al., 2006a; Yamashita et al., 2007; Schindl et al., 2008). Furthermore, it is well established that 2-APB activates Orai3 channels by dilating the pore (Schindl et al., 2008). We hypothesized that pore dilation by 2-APB might allow E165 to move toward the central axis, or pore, of the channel and thereby interact with incoming ions. Store-operated Orai3 channels are not dilated; therefore, we anticipated that E165 would play a lesser role in the formation of the store-operated Orai3 pore, and would therefore not interact with incoming ions during STIM1-induced activation of Orai3. To test this hypothesis, we neutralized the residue and assumed that removing the negative charge might diminish 2-APB–activated, but not store-operated, current densities.

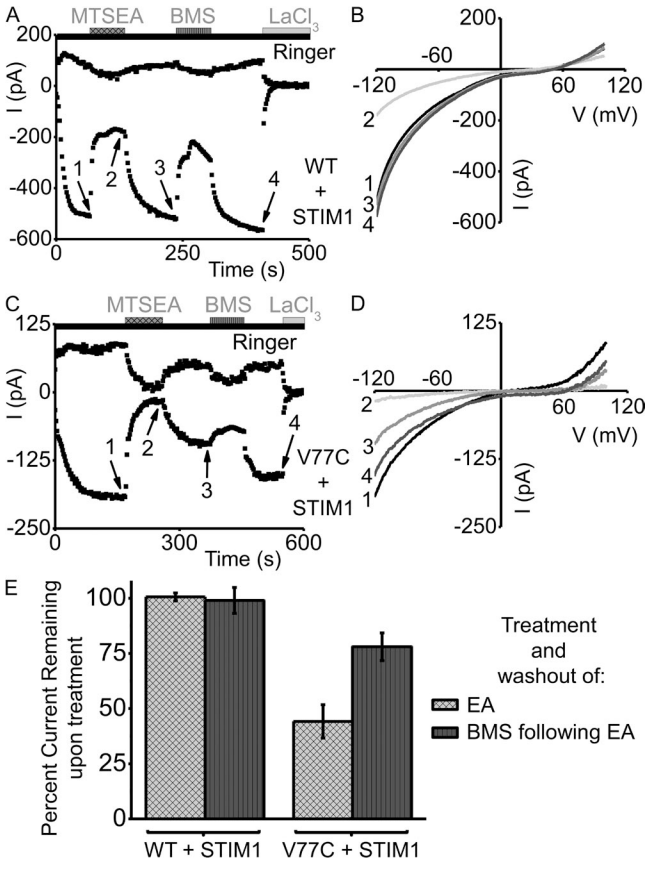

Figure 3. Store-operated Orai3-V77C channels are sensitive to block by MTSEA. (A) Time course for Orai3-WT cotransfected with STIM1 (WT + STIM1; $n = 3$) and activated by passive store depletion, represented as current amplitude (pA) versus time (s). Both MTSEA (EA) and BMS reversibly block Orai3-WT store-operated current. (B) I-V relationships corresponding to currents recorded at time points indicated by the arrows in A. (C) Time course for Orai3-V77C cotransfected with STIM1 (V77C + STIM1; $n = 8$). Block induced by EA is reversed after application of BMS. (D) I-V relationships corresponding to currents recorded at time points indicated by the arrows in C. (E) Bar graphs summarizing the percentage of current amplitude remaining after EA or BMS treatment and washout. Data are normalized to current amplitude before EA application. Error bars indicate SEM.

At first glance, 2-APB–activated Orai3-WT and Orai3-E165A channels appear similar in terms of ion selectivity; both conduct nonselective cationic currents that have inwardly and outwardly rectifying I-V shapes. However, compared with 2-APB–activated Orai3-WT ($n = 7$), expression of Orai3-E165A channels ($n = 7$) resulted in increased Ca^{2+} selectivity and an ~20-fold decrease in 2-APB–activated current density (Fig. 4, A–E). The decrease in current density is reminiscent of mutation E165Q, which also results in decreased 2-APB–activated Orai3 currents (Schindl et al., 2008).

Store-operated Orai3-WT ($n = 6$) and Orai3-E165A ($n = 5$) channels were similar in terms of current density (Fig. 4, F–J). Additionally, neither WT nor mutant channels exhibited increased current amplitudes upon solution exchange from 2 to 20 mM Ca^{2+} Ringer (Fig. 4, F–I). Previous studies have illustrated that both endogenously expressed CRAC channel currents (Bootman et al., 2001; Parekh and Putney, 2005) and heterologously expressed store-operated Orai1 and dOrai channel currents (Yeromin et al., 2004; Zhang et al., 2008) double in amplitude upon external solution exchange from 2 mM to 6–20 mM Ca^{2+}. Hence it is surprising that a similar solution exchange protocol does not increase store-operated Orai3 current amplitude. The result suggests that store-operated Orai3 is not as Ca^{2+} selective as Orai1 or dOrai. Another aspect of the store-operated Orai3-E165A current to be noted is the increased outward component carried by cesium ions (Cs^+; Fig. 4, H–J). This property of the current was not a surprise, as mutating the homologous residue E190 of Orai1 to glutamine also imparts increased Cs^+ permeability (Prakriya et al., 2006; Vig et al., 2006b).

In summary, mutation E165A drastically inhibits 2-APB–activated, but not store-operated, Orai3 current. This result agrees with our earlier hypothesis: residue E165, which is excluded from the store-operated Orai3 pore, can enter and assist in formation of the dilated pore of the 2-APB–activated Orai3 channel.

Orai3-E165C is sensitive to block by $CdCl_2$ when channels are activated by 2-APB

To further test whether residue E165 is involved in formation of the 2-APB–activated Orai3 pore, or if it is

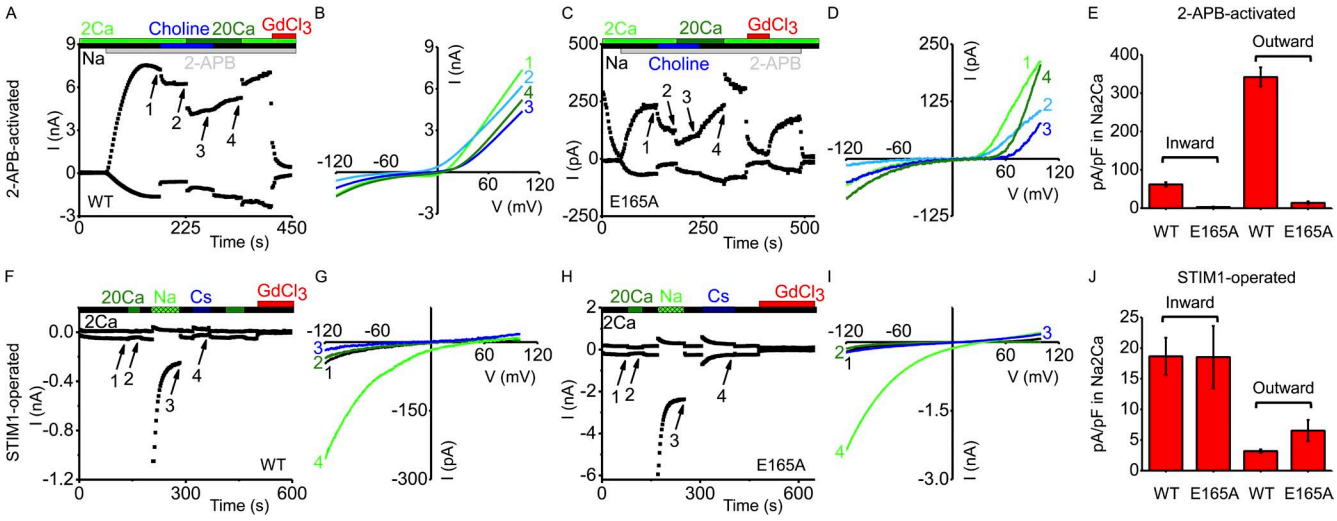

Figure 4. Orai3-E165A exhibits diminished 2-APB–activated, but normal store-operated, current densities. (A) Time course for Orai3-WT (WT; $n = 7$) currents activated by 100 µM 2-APB. (B) I-V relationships corresponding to currents recorded at time points indicated by the arrows in A. (C) Time course for Orai3-E165A (E165A; $n = 7$) currents activated by 100 µM 2-APB. (D) I-V relationships corresponding to currents recorded at time points indicated by the arrows in C. (E) Bar graphs showing ∼20-fold decreased current densities carried by Orai3-E165A channels when activated by 2-APB, as compared with Orai3-WT. (F) Time course for Orai3-WT cotransfected with STIM1 (WT; $n = 6$) and current activated by passive store depletion. (G) I-V relationships corresponding to currents recorded at time points indicated by the arrows in F. (H) Time course for Orai3-E165A cotransfected with STIM1 (E165A; $n = 5$) and current activated by passive store depletion. (G) I-V relationships corresponding to currents recorded at time points indicated by the arrows in H. (F) Summarizing bar graphs show that current density carried by store-operated Orai3-E165A channels is comparable to WT channels. Error bars indicate SEM.

permitted to move toward the central axis of the channel during 2-APB–induced dilation, where it could interact with incoming ions, we sought to evaluate Cd^{2+} block of Orai3-E165C. As shown by representative I-V relationships in Fig. 5 (A and B), 2-APB–activated Orai3-WT channels exhibited a fivefold decrease in sensitivity to $CdCl_2$ block ($n = 10$) as compared with store-operated Orai3-WT channels ($n = 3$). The dilated 2-APB–activated Orai3 channel pore requires greater concentrations of $CdCl_2$ to be blocked. $CdCl_2$ dose–response curves for Orai3-WT channels, activated either by 2-APB or store depletion, are represented in Fig. 5 C. Interestingly, 2-APB–activated Orai3-E165C channels are almost three times more sensitive to $CdCl_2$ block ($n = 6$; Fig. 5, D and F) than Orai3-WT channels, which suggests that a weak interaction occurs between the Cd^{2+} ions and the cysteine mutated into position 165, and that this interaction blocks the conduction pathway of the 2-APB–activated Orai3 channel. Furthermore, although the E165C mutation induces sensitivity to $CdCl_2$ block during 2-APB activation, it does not increase sensitivity to $CdCl_2$ block when the mutant channel is store-operated ($n = 3$; Fig. 5, E and F). In fact, store-operated Orai3-E165C channels are approximately half as sensitive to $CdCl_2$ block as store-operated Orai3-WT channels. $CdCl_2$ dose–response curves for Orai3-E165C channels, activated either by 2-APB or store depletion, are represented in Fig. 5 F. Our data show that mutation E165C results in increased sensitivity to block by $CdCl_2$, but only when Orai3 is 2-APB activated, not store operated. Based on the data presented for both E165A and E165C mutants, we suggest that as 2-APB dilates the Orai3 pore, position 165 becomes exposed to the formed conduction pathway and thus plays a role in pore formation. However, if the channel is store-operated, position 165 is excluded from the conduction pathway, and therefore mutations E165A and E165C have little effect on store-operated Orai3 currents.

Finally, we tested Orai3-E165C for reactivity with MTSEA and MTSET and found that the mutation did not result in irreversible block upon treatment with either MTS reagent (Fig. S3). Perhaps, similar to mutation L70C, E165C induces sensitivity to $CdCl_2$ block but is too deep into the pore or too hindered by surrounding residues to interact with MTS reagents.

DISCUSSION

Previous functional studies have identified conserved Orai1 TM1 residues that are necessary for channel selectivity and gating. Several of the corresponding residues for Orai3 are represented in the homology model (Fig. 6). On the extracellular side of TM1, the selectivity filter residue necessary for Ca^{2+} selectivity was identified as E106 in Orai1 (Prakriya et al., 2006; Vig et al., 2006a; Yeromin et al., 2006) or E81 in Orai3 (Schindl et al., 2008; Demuro et al., 2011). Atop TM1, V102 of Orai1

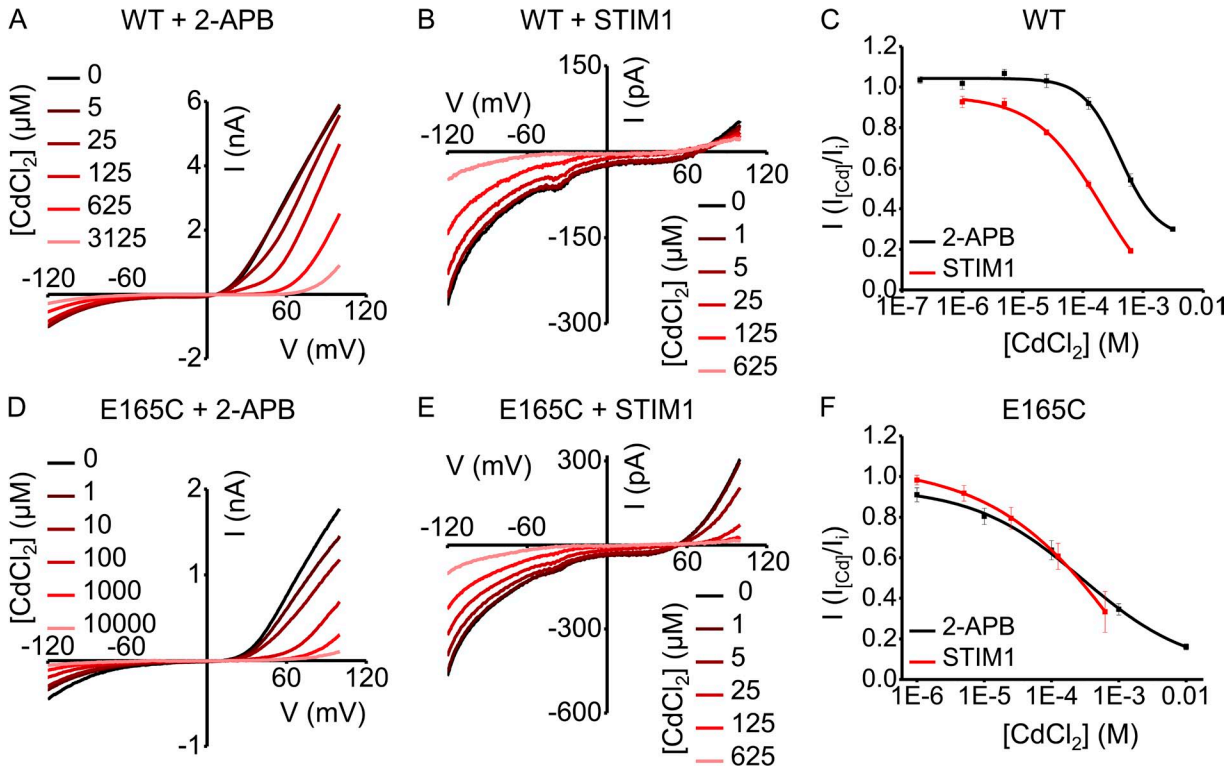

Figure 5. Orai3-E165C is sensitive to block by $CdCl_2$ when channels are activated by 2-APB. (A) I-V relationships for Orai3-WT activated by 100 μM 2-APB (WT + 2-APB; $n = 10$), blocked by increasing concentrations of $CdCl_2$ (from 5 μM to 3.125 mM). (B) I-V relationships for Orai3-WT cotransfected with STIM1 (WT + STIM1; $n = 3$), activated by passive store-depletion, blocked by increasing concentrations of $CdCl_2$ (from 1 to 625 μM). (C) Fraction of 2-APB–activated or STIM1-operated inward current remaining upon applied concentration of $CdCl_2$ in WT channels. Calculated K_d values for $CdCl_2$ block of inward currents carried by 2-APB–activated or STIM1-operated WT channels are as follows: 734 and 137 μM, respectively. The calculated K_d value for $CdCl_2$ block of outward currents carried by 2-APB–activated WT channels is 549 μM. Points are data gathered from experiments represented in A and B, and curves are sigmoidal fits of data, represented as $I_{[Cd]}/I_i$, where $I_{[Cd]}$ is current recorded after application of $CdCl_2$ and I_i is current recorded before application of $CdCl_2$. (D) I-V relationships for Orai3-E165C activated by 100 μM 2-APB (E165C + 2-APB; $n = 6$) and blocked by increasing concentrations of $CdCl_2$ (from 1 μM to 10 mM). (E) I-V relationships for Orai3-E165C cotransfected with STIM1 (E165C + STIM1; $n = 3$), activated by passive store depletion, and blocked by increasing concentrations of $CdCl_2$ (from 1 to 625 μM). (F) Fraction of 2-APB–activated or STIM1-operated inward current remaining upon applied concentration of $CdCl_2$ to E165C channels. Calculated K_d values for $CdCl_2$ block of inward currents carried by 2-APB–activated or STIM1-operated E165C channels are as follows: 275 and 246 μM, respectively. The calculated K_d value for $CdCl_2$ block of outward currents carried by 2-APB–activated E165C channels is 130 μM. Points are data gathered from experiments represented in D and E, and curves are sigmoidal fits of data, represented as $I_{[Cd]}/I_i$, where $I_{[Cd]}$ is the current recorded after application of $CdCl_2$ and I_i is the current recorded before application of $CdCl_2$. Error bars indicate SEM.

(V77 in Orai3) has been shown to function as a hydrophobic gate; mutation V102C results in constitutively active Orai1 channels (McNally et al., 2012). At the center of TM1, G98 of Orai1 (G73 in Orai3) is required for normal STIM-induced gating. A gating-hinge mechanism was proposed by Zhang et al. (2011). Near the intracellular side of TM1, R91 in Orai1 (R66 in Orai3) contributes to the formation of a narrow and highly basic "gate" that generates an electrostatic barrier so that Ca^{2+} ions cannot pass (Feske et al., 2006; Derler et al., 2009; Zhang et al., 2011). Hence, when R91 is mutated to bulky hydrophobic residues, the channel is blocked. Accordingly, cysteine scanning mutagenesis studies performed on store-operated Orai1 (McNally et al., 2009; Zhou et al., 2010) and the published crystal structure of a homologous, hypothetically closed state, dOrai (Hou et al., 2012), showed that TM1 residues from top to bottom are involved in pore formation.

Aside from TM1, additional functional studies have identified Orai1 and Orai3 TM3 residues that are necessary for channel selectivity and gating. Toward the extracellular side of TM3, E190 of Orai1 or E165 of Orai3 (shown in the homology model; Fig. 6) also contribute to Ca^{2+} selectivity. Orai1 mutation E190Q or Orai3 mutation E165Q result in an altered I-V relationship characteristic of increased Cs^+ permeability (Prakriya et al., 2006; Vig et al., 2006a; Yamashita et al., 2007; Schindl et al., 2008). At the center of TM3, G183 in Orai1 (G158 of Orai3) is required for normal STIM-induced gating and 2-APB activation. Orai1 mutation G183A confers 2-APB sensitivity (Srikanth et al., 2011), whereas Orai3 mutation G158C results in slow kinetics of 2-APB activation

and washout due to disulfide bridge formation between the introduced G158C and endogenous TM2 C101 (Amcheslavsky et al., 2013). However, the aforementioned cysteine scanning studies and the dOrai crystal structure did not identify these TM3 residues as necessary for Orai channel pore formation. In particular, no hypotheses have been made or mechanisms discovered for how the TM3 glutamate might affect Ca^{2+} selectivity.

Therefore, from a structural point of view, the functional contributions of this conserved TM3 glutamate (E190 in Orai1, E165 in Orai3) were left unexplained. Furthermore, the 2-APB–activated Orai3 channel pore, dilated and therefore nonselective, characterized by a biphasic I-V shape with inward and outward rectification, has not been examined. In this study, we have sought to further the structural understanding of Orai channels by applying targeted cysteine mutagenesis, thiol-reactive reagents, and patch clamp analysis, to 2-APB–activated Orai3.

Our study probes the 2-APB–activated Orai3 channel pore by cysteine mutagenesis at several sites in TM1 and at E165 of TM3. We show that 2-APB–activated Orai3-WT channels require greater concentrations of $CdCl_2$ to block current than do store-operated Orai3 (Fig. 5) or Orai1 channels (McNally et al., 2009). Furthermore, although Orai3 mutants E81C, G73A, G73C, and R66C did not form channels capable of conducting in response to 2-APB stimulation (Fig. S1), Orai3 mutants Q83C, V77C, L70C, E165A, and E165C provide insight into the structural makeup of the 2-APB–activated Orai3 channel pore. To illustrate this, we have transposed Orai3 residues Q83, V77, L70C, and E165, along with selectivity filter residue E81 for reference, onto the dOrai crystal structure (Fig. 6).

Structural insights from Orai3 TM1 cysteine mutants: Block by $CdCl_2$ and MTSEA

Of the four residues studied in detail, Q83 is the most extracellular, positioned just above selectivity filter E81 (Fig. 6, A, B, and F). Orai3-Q83C channels are sensitive to block by Cd^{2+} ions; however, current amplitudes rise instantly upon washout of applied $CdCl_2$ (Fig. 1). Furthermore, MTS reagents do not induce block of 2-APB–activated current carried by Orai3-Q83C channels (Fig. S2, C–H). We suggest that although position 83 lies above the pore, it is not directly within the pore, and therefore covalent interaction between Q83C and MTS reagents would not result in drastic block of current. Instead, a covalently linked MTS reagent would only create a small steric hindrance to ions as they enter the conduction pathway of 2-APB–activated Orai3.

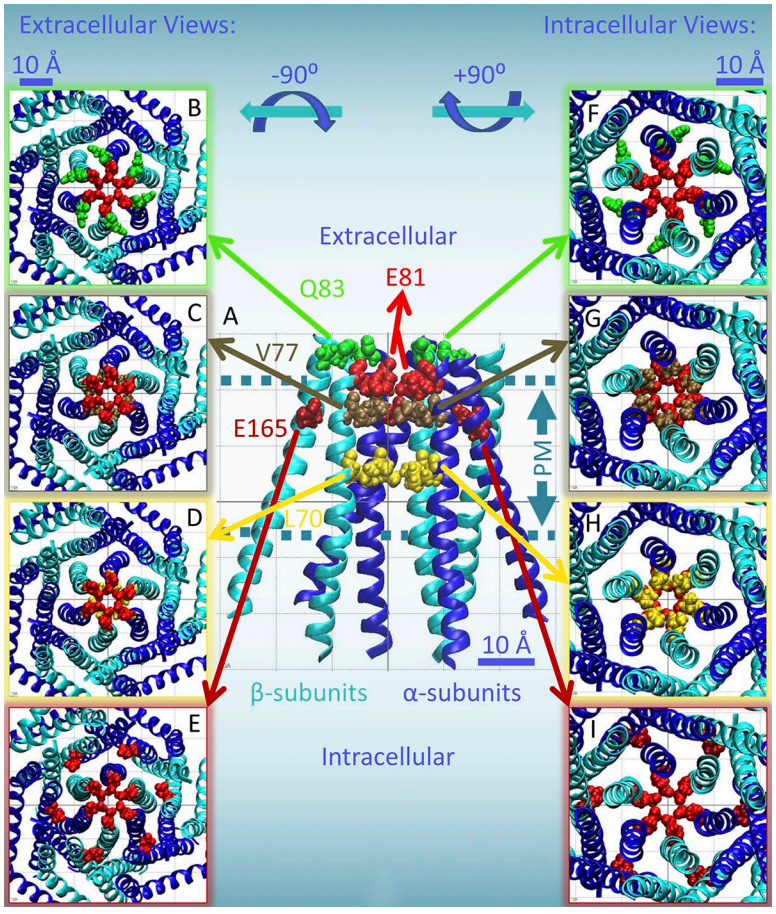

Figure 6. Structural insight into the Orai3 pore. (A) Orai3 residues examined in this study (Q83, green; V77, brown; L70, yellow; and E165, burgundy), along with the E81 selectivity filter (red) for reference, transposed onto the closed state dOrai crystal structure. For visual clarity, only TM1 and TM3 domains are shown and only four of the six subunits in the crystal structure are represented. α Subunits appear in blue and β subunits in turquoise. Boundaries of the PM are represented as blue dotted lines. (B–E) Images displaying extracellular views of the entire crystallized dOrai channel. In each image, only two Orai3 residues are transposed onto the dOrai crystal structure: E81 and either Q83, V77, L70, or E165. Note that only Q83 (B) and E165 (E) are visible and that V77 (C) and L70 (D) are deeper in the pore, more intracellular than E81. Q83 does not directly align with the central axis of the channel. E165 of TM3 is directly behind and in between two TM1 domains. (F–I) Images displaying intracellular views of the entire crystallized dOrai channel. In each image, only two Orai3 residues are transposed onto the dOrai crystal structure: E81 and Q83, V77, L70, or E165. Note that in this view of the channel, Q83 is hidden behind E81 (F), V77 is very closely positioned to and aligns well with E81 (G), L70 is deeper in the pore (H), and E165 can be seen behind and between TM1 domains (I). The dilated open 2-APB–activated Orai3 channel allows cysteine mutants Q83C, V77C, L70C, and E165C to interact with incoming Cd^{2+} ions. The interactions between E165C and Cd^{2+} ions only exists when the channel is 2-APB activated, not store operated. Mutant V77C also renders the open state of the channel sensitive to block by MTSEA.

We found that Orai3-V77C channels are highly sensitive to block by Cd^{2+} ions, more so than Q83C, L70C, or E165C mutant channels (Figs. 1 and 5). Furthermore, both 2-APB–activated and store-operated Orai3-V77C channels are sensitive to block by MTSEA (Figs. 2 and 3), and MTSEA-induced block is state-dependent, as MTSEA fails to block Orai3-V77C before channel opening (Fig. 2). The fact that MTSEA blocks 2-APB–activated Orai3 channels is consistent with dilation of the 2-APB–activated Orai3 channel pore, resulting in a nonselective and wider open channel than store-operated Orai channels. Furthermore, V77 is perfectly positioned at the central axis of the channel, just underneath selectivity filter E81 (Fig. 6, A, C, and G), and its reaction with MTSEA would form a plug that could directly inhibit conduction. However, MTSEA block of store-operated Orai3-V77C came as a surprise, as MTS reagents are unable to penetrate the narrow, Ca^{2+} selective, store-operated Orai1 pore (McNally et al., 2009). The only Orai1 cysteine mutant able to interact with MTSEA has a dilated pore induced by secondary mutation to selectivity filter E106 (Orai1-E106D/G98C; McNally et al., 2012). Because position V77 is more intracellular than the selectivity filter E81, and yet Orai3-V77C channels lacking the secondary homologous E81D mutation are able to interact with MTSEA to induce irreversible, state-dependent channel block, we suggest that store-operated Orai3 channels do in fact have wider pores than store-operated Orai1 channels. Finally, Orai3-V77C channels and homologous Orai1-V102C mutant channels have been reported to conduct preactivated, nonselective currents (McNally et al., 2012). In our hands, Orai3-V77C channels were not preactivated.

Position L70 in TM1 is even deeper in the pore than V77 (Fig. 6, A, D, and H). Although Orai3-L70C mutant channels are more sensitive to block by Cd^{2+} than are Orai3-WT channels, they do not exhibit MTS reagent-induced irreversible block of 2-APB–activated current (Fig. S2, I and J). Perhaps L70C is too deep into the pore or is hindered by bulkier, more extracellular residues, such as F74, to be reached by bulkier MTS reagents.

Our data show that the 2-APB–activated Orai3 pore is lined by at least three TM1 residues: Q83, V77, and L70. The remaining TM1 cysteine mutants we tested, E81C, G73C, and R66C, lost sensitivity to activation by 2-APB. Therefore, we cannot say with certainty whether these residues are involved in the formation of the 2-APB–activated Orai3 pore. However, because E81 forms the selectivity filter, we conclude that Q83, E81, V77, and L70 are all involved in the formation of the 2-APB–activated pore.

Structural insights from state-dependent effects of Orai3 TM3 E165 mutants

The state-dependent effects of Orai3 TM3 mutations illustrate how the 2-APB–activated pore might differ from the store-operated pore. The E165A mutation diminishes 2-APB–activated Orai3 current densities; however, it does not alter current density carried by store-operated Orai3 channels (Fig. 4). Furthermore, position 165 within the Orai3 channel, as predicted by the dOrai crystal structure (Fig. 6, A, E, and I), is located directly behind and in between two TM1 pore-forming helices. We hypothesized that during 2-APB–induced pore dilation, position 165 might move toward the central axis of the channel, thus affecting the channel's permeation properties. Perhaps mutation E165A inhibits proper formation of the dilated 2-APB–activated Orai3 pore. The store-operated pore, known to exclude TM3 residues from the conduction pathway, would exclude E165 from the TM1-comprised conduction pathway, and thus mutation E165A would have little effect on store-operated pore formation or current density. Consistent with this hypothesis, mutation E165C increased Cs^{+} permeability through the store-operated Orai3 pore, but did not increase sensitivity to $CdCl_2$ block. In fact, compared with store-operated Orai3-WT channels, store-operated Orai3-E165C channels were approximately two times less sensitive to block by $CdCl_2$. However, 2-APB–activated Orai3-E165C channels were almost three times more sensitive to block by $CdCl_2$ than were 2-APB–activated Orai3-WT channels (Fig. 5). Our data suggest that E165C is able to penetrate the 2-APB–activated Orai3 conduction pathway and thus is able to interact with incoming Cd^{2+} ions. Comparing state-dependent effects of mutations E165A and E165C on 2-APB–activated and store-operated Orai3 currents leads us to conclude that position 165 within Orai3 moves toward the central axis of the channel and therefore assists in pore formation, but only when the channel is activated and dilated by 2-APB.

This work is supported by National Institutes of Health grant NS-14609 to M.D. Cahalan.

The authors declare no competing financial interests.

Sharona E. Gordon served as editor.

Submitted: 23 January 2014
Accepted: 24 March 2014

REFERENCES

Amcheslavsky, A., O. Safrina, and M.D. Cahalan. 2013. Orai3 TM3 point mutation G158C alters kinetics of 2-APB-induced gating by disulfide bridge formation with TM2 C101. *J. Gen. Physiol.* 142: 405–412. http://dx.doi.org/10.1085/jgp.201311030

Bootman, M.D., P. Lipp, and M.J. Berridge. 2001. The organisation and functions of local Ca^{2+} signals. *J. Cell Sci.* 114:2213–2222.

Cahalan, M.D. 2009. STIMulating store-operated Ca^{2+} entry. *Nat. Cell Biol.* 11:669–677. http://dx.doi.org/10.1038/ncb0609-669

DeHaven, W.I., J.T. Smyth, R.R. Boyles, G.S. Bird, and J.W. Putney Jr. 2008. Complex actions of 2-aminoethyldiphenyl borate on store-operated calcium entry. *J. Biol. Chem.* 283:19265–19273. http://dx.doi.org/10.1074/jbc.M801535200

Demuro, A., A. Penna, O. Safrina, A.V. Yeromin, A. Amcheslavsky, M.D. Cahalan, and I. Parker. 2011. Subunit stoichiometry of human Orai1 and Orai3 channels in closed and open states. *Proc. Natl. Acad. Sci. USA.* 108:17832–17837. http://dx.doi.org/10.1073/pnas.1114814108

Derler, I., M. Fahrner, O. Carugo, M. Muik, J. Bergsmann, R. Schindl, I. Frischauf, S. Eshaghi, and C. Romanin. 2009. Increased hydrophobicity at the N terminus/membrane interface impairs gating of the severe combined immunodeficiency-related ORAI1 mutant. *J. Biol. Chem.* 284:15903–15915. http://dx.doi.org/10.1074/jbc.M808312200

Feske, S., Y. Gwack, M. Prakriya, S. Srikanth, S.H. Puppel, B. Tanasa, P.G. Hogan, R.S. Lewis, M. Daly, and A. Rao. 2006. A mutation in Orai1 causes immune deficiency by abrogating CRAC channel function. *Nature.* 441:179–185. http://dx.doi.org/10.1038/nature04702

Hou, X., L. Pedi, M.M. Diver, and S.B. Long. 2012. Crystal structure of the calcium release-activated calcium channel Orai. *Science.* 338:1308–1313. http://dx.doi.org/10.1126/science.1228757

Liou, J., M.L. Kim, W.D. Heo, J.T. Jones, J.W. Myers, J.E. Ferrell Jr., and T. Meyer. 2005. STIM is a Ca^{2+} sensor essential for Ca^{2+}-store-depletion-triggered Ca^{2+} influx. *Curr. Biol.* 15:1235–1241. http://dx.doi.org/10.1016/j.cub.2005.05.055

Lioudyno, M.I., J.A. Kozak, A. Penna, O. Safrina, S.L. Zhang, D. Sen, J. Roos, K.A. Stauderman, and M.D. Cahalan. 2008. Orai1 and STIM1 move to the immunological synapse and are up-regulated during T cell activation. *Proc. Natl. Acad. Sci. USA.* 105:2011–2016. http://dx.doi.org/10.1073/pnas.0706122105

Lis, A., C. Peinelt, A. Beck, S. Parvez, M. Monteilh-Zoller, A. Fleig, and R. Penner. 2007. CRACM1, CRACM2, and CRACM3 are store-operated Ca^{2+} channels with distinct functional properties. *Curr. Biol.* 17:794–800. http://dx.doi.org/10.1016/j.cub.2007.03.065

McNally, B.A., M. Yamashita, A. Engh, and M. Prakriya. 2009. Structural determinants of ion permeation in CRAC channels. *Proc. Natl. Acad. Sci. USA.* 106:22516–22521. http://dx.doi.org/10.1073/pnas.0909574106

McNally, B.A., A. Somasundaram, M. Yamashita, and M. Prakriya. 2012. Gated regulation of CRAC channel ion selectivity by STIM1. *Nature.* 482:241–245.

Parekh, A.B., and J.W. Putney Jr. 2005. Store-operated calcium channels. *Physiol. Rev.* 85:757–810. http://dx.doi.org/10.1152/physrev.00057.2003

Peinelt, C., A. Lis, A. Beck, A. Fleig, and R. Penner. 2008. 2-Aminoethoxydiphenyl borate directly facilitates and indirectly inhibits STIM1-dependent gating of CRAC channels. *J. Physiol.* 586:3061–3073. http://dx.doi.org/10.1113/jphysiol.2008.151365

Prakriya, M., S. Feske, Y. Gwack, S. Srikanth, A. Rao, and P.G. Hogan. 2006. Orai1 is an essential pore subunit of the CRAC channel. *Nature.* 443:230–233. http://dx.doi.org/10.1038/nature05122

Putney, J.W., Jr. 1986. A model for receptor-regulated calcium entry. *Cell Calcium.* 7:1–12. http://dx.doi.org/10.1016/0143-4160(86)90026-6

Roos, J., P.J. DiGregorio, A.V. Yeromin, K. Ohlsen, M. Lioudyno, S. Zhang, O. Safrina, J.A. Kozak, S.L. Wagner, M.D. Cahalan, et al. 2005. STIM1, an essential and conserved component of store-operated Ca^{2+} channel function. *J. Cell Biol.* 169:435–445. http://dx.doi.org/10.1083/jcb.200502019

Schindl, R., J. Bergsmann, I. Frischauf, I. Derler, M. Fahrner, M. Muik, R. Fritsch, K. Groschner, and C. Romanin. 2008. 2-aminoethoxydiphenyl borate alters selectivity of Orai3 channels by increasing their pore size. *J. Biol. Chem.* 283:20261–20267. http://dx.doi.org/10.1074/jbc.M803101200

Soboloff, J., B.S. Rothberg, M. Madesh, and D.L. Gill. 2012. STIM proteins: dynamic calcium signal transducers. *Nat. Rev. Mol. Cell Biol.* 13:549–565. http://dx.doi.org/10.1038/nrm3414

Srikanth, S., M.K. Yee, Y. Gwack, and B. Ribalet. 2011. The third transmembrane segment of orai1 protein modulates Ca^{2+} release-activated Ca^{2+} (CRAC) channel gating and permeation properties. *J. Biol. Chem.* 286:35318–35328. http://dx.doi.org/10.1074/jbc.M111.265884

Vig, M., A. Beck, J.M. Billingsley, A. Lis, S. Parvez, C. Peinelt, D.L. Koomoa, J. Soboloff, D.L. Gill, A. Fleig, et al. 2006a. CRACM1 multimers form the ion-selective pore of the CRAC channel. *Curr. Biol.* 16:2073–2079. http://dx.doi.org/10.1016/j.cub.2006.08.085

Vig, M., C. Peinelt, A. Beck, D.L. Koomoa, D. Rabah, M. Koblan-Huberson, S. Kraft, H. Turner, A. Fleig, R. Penner, and J.P. Kinet. 2006b. CRACM1 is a plasma membrane protein essential for store-operated Ca^{2+} entry. *Science.* 312:1220–1223. http://dx.doi.org/10.1126/science.1127883

Yamashita, M., L. Navarro-Borelly, B.A. McNally, and M. Prakriya. 2007. Orai1 mutations alter ion permeation and Ca^{2+}-dependent fast inactivation of CRAC channels: evidence for coupling of permeation and gating. *J. Gen. Physiol.* 130:525–540. http://dx.doi.org/10.1085/jgp.200709872

Yamashita, M., A. Somasundaram, and M. Prakriya. 2011. Competitive modulation of Ca^{2+} release-activated Ca^{2+} channel gating by STIM1 and 2-aminoethyldiphenyl borate. *J. Biol. Chem.* 286:9429–9442. http://dx.doi.org/10.1074/jbc.M110.189035

Yeromin, A.V., J. Roos, K.A. Stauderman, and M.D. Cahalan. 2004. A store-operated calcium channel in *Drosophila* S2 cells. *J. Gen. Physiol.* 123:167–182. http://dx.doi.org/10.1085/jgp.200308982

Yeromin, A.V., S.L. Zhang, W. Jiang, Y. Yu, O. Safrina, and M.D. Cahalan. 2006. Molecular identification of the CRAC channel by altered ion selectivity in a mutant of Orai. *Nature.* 443:226–229. http://dx.doi.org/10.1038/nature05108

Zhang, S.L., Y. Yu, J. Roos, J.A. Kozak, T.J. Deerinck, M.H. Ellisman, K.A. Stauderman, and M.D. Cahalan. 2005. STIM1 is a Ca^{2+} sensor that activates CRAC channels and migrates from the Ca^{2+} store to the plasma membrane. *Nature.* 437:902–905. http://dx.doi.org/10.1038/nature04147

Zhang, S.L., J.A. Kozak, W. Jiang, A.V. Yeromin, J. Chen, Y. Yu, A. Penna, W. Shen, V. Chi, and M.D. Cahalan. 2008. Store-dependent and -independent modes regulating Ca^{2+} release-activated Ca^{2+} channel activity of human Orai1 and Orai3. *J. Biol. Chem.* 283:17662–17671. http://dx.doi.org/10.1074/jbc.M801536200

Zhang, S.L., A.V. Yeromin, J. Hu, A. Amcheslavsky, H. Zheng, and M.D. Cahalan. 2011. Mutations in Orai1 transmembrane segment 1 cause STIM1-independent activation of Orai1 channels at glycine 98 and channel closure at arginine 91. *Proc. Natl. Acad. Sci. USA.* 108:17838–17843. http://dx.doi.org/10.1073/pnas.1114821108

Zhou, Y., S. Ramachandran, M. Oh-Hora, A. Rao, and P.G. Hogan. 2010. Pore architecture of the ORAI1 store-operated calcium channel. *Proc. Natl. Acad. Sci. USA.* 107:4896–4901. http://dx.doi.org/10.1073/pnas.1001169107